IOPscience iopscience.iop.org

Home Search Collections Journals About Contact us My IOPscience

A self-regulating valve for single-phase liquid cooling of microelectronics

This article has been downloaded from IOPscience. Please scroll down to see the full text article.

2011 J. Micromech. Microeng. 21 104010

(http://iopscience.iop.org/0960-1317/21/10/104010)

View the table of contents for this issue, or go to the journal homepage for more

Download details:
IP Address: 134.58.253.57
The article was downloaded on 30/09/2011 at 09:47

Please note that terms and conditions apply.

J. Micromech. Microeng. **21** (2011) 104010 (11pp) doi:10.1088/0960-1317/21/10/104010

A self-regulating valve for single-phase liquid cooling of microelectronics

Radu Donose, Michaël De Volder, Jan Peirs and Dominiek Reynaerts

Departement Werktuigkunde, Katholieke Universiteit Leuven, Leuven, Belgium

E-mail: Radu.Donose@mech.kuleuven.be

Received 1 April 2011, in final form 22 July 2011
Published 29 September 2011
Online at stacks.iop.org/JMM/21/104010

Abstract

This paper reports on the design, optimization and testing of a self-regulating valve for single-phase liquid cooling of microelectronics. Its purpose is to maintain the integrated circuit (IC) at constant temperature and to reduce power consumption by diminishing flow generated by the pump as a function of the cooling requirements. It uses a thermopneumatic actuation principle that combines the advantages of zero power consumption and small size in combination with a high flow rate and low manufacturing costs. The valve actuation is provided by the thermal expansion of a liquid (actuation fluid) which, at the same time, actuates the valve and provides feed-back sensing. A maximum flow rate of 38 kg h^{-1} passes through the valve for a heat load up to 500 W. The valve is able to reduce the pumping power by up to 60% and it has the capability to maintain the IC at a more uniform temperature.

(Some figures in this article are in colour only in the electronic version)

1. Introduction

During operation, integrated circuits (ICs) produce excess heat, which must be dissipated or absorbed by cooling devices to avoid overheating. Thermal fluctuation is one of the main issues for electronic lifetime [1–3] and, therefore, improved chip cooling results in both increased performance and enhanced reliability of the IC. Cycles of alternating temperatures lead to repeated changes in dimension of electronic components which then lead to the shortening of their lifetime. However, most electronics cooling solutions [4, 5] consume power. In many cases this energy consumption is not optimized, being wasted on excess cooling [6].

In this work, we present a thermopneumatic valve that targets these issues. It is designed to both decrease temperature fluctuations and reduce the cooling power consumption. This is achieved by actively controlling the flow delivered by the pump as a function of the cooling requirements.

In the design of our system, a thermo-fluidic model is used as a first-order tool for global system simulation, including variables such as pressure drop, mass flow, temperature, coolant properties and basic geometrical properties. The model is based on analytical calculations, using design methodologies for efficient heat transfer in microsystems, described in detail in a former publication [7]. The model is implemented in Matlab and used to justify usage of valves in single-phase flow systems, and to investigate the effect of flow control on the cooling performance for multiple chip/heat sink pairs. The developed system is designed to meet typical cooling requirements of an IC 1 cm^2 in size, by absorbing up to 500 W cm^{-2} at a temperature difference of 35–40 °C. The temperature difference is defined between the maximum junction temperature (at the end of the channels) and the inlet temperature of the coolant. To achieve these high performances, conventional air-cooling is not sufficient and therefore liquid cooling is used. Water is selected as coolant because of its excellent heat capacity. During the passage through the heat sink, the coolant remains in the liquid phase, hence the name ‘single-phase cooling’. This is in contrast to systems where the coolant is allowed to evaporate in the heat sink to form a two-phase mixture of liquid and vapour (two-phase cooling).

The flow control is performed by valves in each branch of the circuit, as shown in figure 1. The primary effect of the operation of valves is the reduction of mass flow in a certain branch when the IC in that branch is not working at full load. In this way, we hope to reduce the thermal fluctuations of the IC together with the mass flow and thereby the power required to pump the coolant through the circuit.

In figure 2, the pumping power can be seen with (dashed line) and without (continuous line) control valves as a function

 © 2011 IOP Publishing Ltd Printed in the UK & the USA

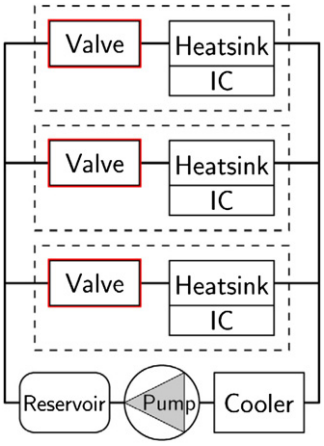

Figure 1. Schematic of the cooling system using valves in each branch of the circuit.

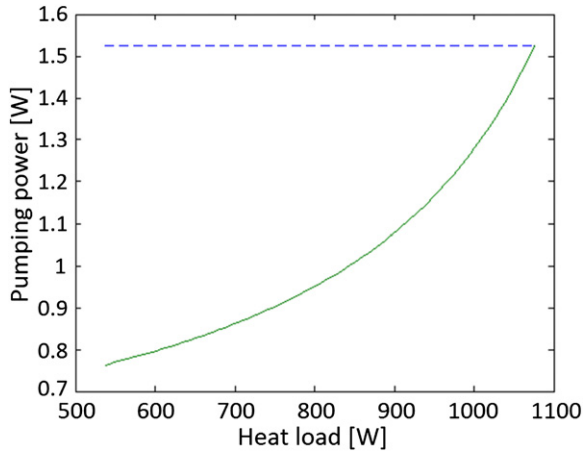

Figure 2. Simulated pumping power versus heat load without (dashed line) and with (continuous line) valve control action.

of heat load, as was determined by the thermo-fluidic model. The simulation was performed for the case of 10 ICs, 5 of them operating at full load and the other 5 operating at partial load from 0 to 100%. As can be seen, the power saving that can be obtained makes the research towards microvalves for single-phase flow valuable.

The literature offers a wide selection of microvalves with numerous actuation mechanisms [8]. To select the best actuation principle for the given requirements several actuation principles were considered including electromagnetic [9], electrostatic, piezoelectric [10] and shape memory alloy [11–15] actuation. Control fluids like magneto/electrorheologic [16], ferrofluids [17, 18] and hydrogels [19, 20] were also considered. Hydraulic and pneumatic actuators deliver among the highest force and power densities at microscale [21]. In comparison with other actuation principles, pneumatic and hydraulic systems offer clear advantages in applications that require low-cost, compliant or high-force actuators [21]. Table 1 summarizes the main characteristics of the above actuators for application in chip cooling valves.

Here thermopneumatic actuation was selected because it offers the ability to capture the thermal waste energy of the IC, converting it to mechanical actuation. It is based on

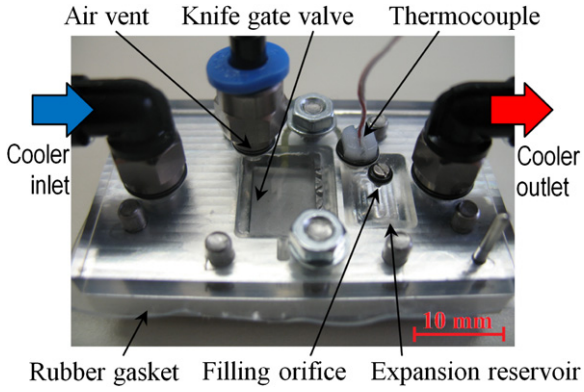

Figure 3. Assembled thermopneumatic valve.

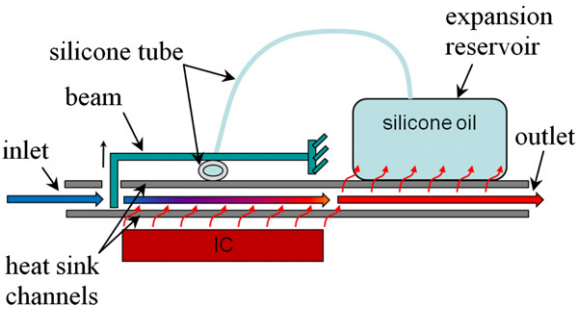

Figure 4. Thermopneumatic valve mechanism.

thermal expansion of a medium by the heat absorbed from the IC. This leads to a valve that consumes no external power and requires no control or electronics, greatly reducing the complexity and the costs. The resulting prototype is shown in figures 3 and 5.

The next section describes the design and operating principle of the valve, with more details provided on the design and assembly of the different valve components. Section 3 describes the fabrication technology, with emphasis on the dimensioning and functionality of each component as well as the fabrication techniques. Section 4 describes the measurement setup, while section 5 covers the actual measurements and the respective interpretations. Results are presented for beam actuation, pressure drop influence on beam position, valve flow rate regulation as function of temperature, valve response time, valve influence on heater (IC) temperature, pumping power savings and pressure drop across the valve.

2. Design and operating principle

The design of the valve is based on the following concepts and ideas:

(1) To make it suitable for portable devices, the valve features a very compact planar design [22].
(2) To reduce the actuation force, the knife-gate principle is adopted [23]: the flow is obstructed by a thin blade, moving perpendicularly to the flow direction, such that the pressure difference across the valve has a minimal

Table 1. Characteristics of various actuator types for application in chip cooling valves.

Characteristics actuation type	Price	Power	Response time	Stroke
Electrostatic	Low	Low	Fast	Very low
Electromagnetic	High	High	Fast	High
Piezoelectric membrane	Low	Low	Fast	Low
Piezostack	Very high	Low	Fast	Very low
Bimetallic	Low	None (passive) High (active)	Slow	High
Thermo-pneumatic	Low	None (passive) High (active)	Slow	High
SMA actuation	Low	None (passive) High (active)	Slow	Low (wire) High (spring)

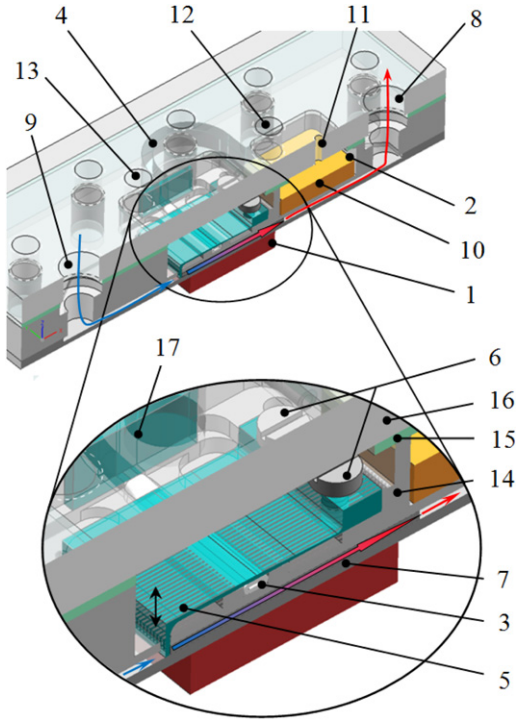

Figure 5. Section view of the thermopneumatic valve.

effect on the actuation force. This principle provides high flow capacity and minimum pressure drop across the valve in the open state.

(3) The response of the valve to the IC temperature is provided by the thermal expansion of a liquid that is heated by the IC. This results in a passive valve which requires no control or external power supply.

Silicone oil is chosen as expansion fluid because it possesses one of the highest expansion coefficients among the non-toxic, inflammable liquids. The silicone oil used (Dow Corning 200 fluid 500 CS) has a volumetric expansion coefficient of 0.96×10^{-3} K^{-1} at 20 °C, which is 4.7 times higher than the expansion of water and 28% higher than the expansion of ethanol.

2.1. Valve operating principle

A schematic representation of the valve mechanism is shown in figure 4. A heat sink is placed over an IC to remove the heat. During operation, the heat generated by the IC is transmitted by the cooling liquid to a down-stream reservoir filled with silicone oil. The latter expands thermally upon increasing temperature and drives the beam of the knife gate valve upwards. This opens the cooling channels which increase the water flow reducing the IC temperature. In other words, this approach provides a temperature feedback system where no temperature sensor or controllers are needed since these are inherently embedded in the system. This results in a passive, cost effective and robust cooling system.

2.2. Detailed valve design

Figure 5 depicts a cross-sectional view of the actual valve design. The heat generated by the IC (1) is transmitted to the silicone oil in the reservoir (2). The silicone oil expands into a silicone tube (3) through a connection channel (4). When the silicone tube is pressing against the beam (5), which is fixed on the frame by screws (6), the beam moves upwards and allows the cooling fluid to enter the heat sink (7) at an increased rate. The heated fluid is leaving the system through the outlet (8) while cold fluid is getting in through the inlet (9). The temperature range in which the valve is sensitive is adjusted by calibre plates (10) of different thicknesses that are inserted in the reservoir replacing a specific quantity of silicone oil. The reservoir is filled through orifice (11). Orifice (12) is used as a port for a temperature or pressure sensor, and orifice (13) to remove the air trapped in the beam enclosure. A silicone membrane (15) provides sealing between the main valve body (14) and the transparent cover (16).

The active parts of the valve consist of the actuating tube (3) and a cantilever-beam that opens and closes the knife-gate valve (5). To amplify the stroke, the tube is placed halfway the beam. The valve controls the cooling fluid at the entrance of the channels for better hydrodynamic stability.

2.3. Beam geometry optimization

The cross-section of the beam (figure 6) is carefully chosen to maximize the deflection range. An important issue is that the flow pressure difference, displayed by the force F_0, acting perpendicularly on the frontal surface of the beam gate (segment A-B) is creating a moment M_0 acting against the moment M developed by the tube, that bends the beam downwards, thus against the normal actuation direction. Therefore, a thicker section was selected for the front part of the beam (A-B-C) to minimize the downward bending effect

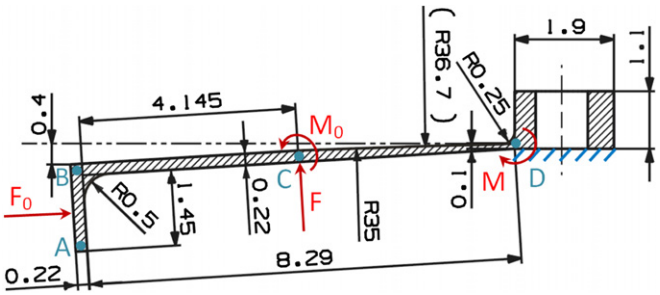

Figure 6. Cross-section of the designed beam.

of the flow pressure, while a thinner section was chosen close to the fixation area (segment C-D) to increase the upward flexing of the beam when intentionally actuated by the tube (force F). The optimization had as fixed constraints the length of the beam segments A-B and B-D and the location of point C. The variables to be optimized were the thickness of these segments as well as the radius of the beam suspension in point D. The analysis of the different beam geometries was performed by means of finite element models (FEMs). The scenarios were selected manually, thus not by a specific optimization algorithm. The best design was defined as the one having the smallest influence of the flow pressure on the beam, resulting in a deflection of 109 μm, or 22% of the net actuation (500 μm). The resulting optimum dimensions are displayed in figure 6.

According to the FEM calculations, a Von-Mises stress of 401 MPa is obtained for a displacement of 900 μm at the gate tip from which 400 μm is used to pre-stress the tube and 500 μm for actuation. The tube force required to reach the full stroke of 500 μm is 1.84 N. If at the same time the maximum flow pressure difference of 0.5 bar is applied, the required tube force rises to 2.07 N. The maximum Von-Mises stress in the beam rises to 418 MPa, compared to the 503 MPa yield stress of the beam material (Al7075).

2.4. Thermopneumatic reservoir

To obtain maximal sensitivity to temperature change, the reservoir is placed over the heat sink at the end of the channels, as close as possible to the IC. This way the heat is directly transported from the heat sink to the reservoir which controls the valve. The wall thickness between the reservoir and the heat sink must be as small as possible to improve heat transfer. This thickness is 0.5 mm.

The volume of silicone oil required for actuation was calculated as a function of the volumetric change of the tube, since it goes from a flattened to a round shape when actuating the beam. Also, the thermal expansion and the inflation of the tube with increasing internal pressure are taken into account. The required reservoir volume V to lift the beam as a function of the temperature difference ΔT is listed in table 2. Here, this volume was adapted by inserting calibre volumes in the reservoir. In an industrial design, the volume is adapted to the work load of a specific IC.

Table 2. Required reservoir volume as a function of temperature difference.

Temperature difference (°C)	Volume (mm^3)
10	350
20	175
30	117
40	88
50	71
60	59

2.5. Heat sink channel aspect ratio optimization

The heat sink geometry is optimized towards minimal thermal resistance, within the limitations of the manufacturing tools available on the market. First, the frictional pressure drop Δp_f is calculated to obtain the relation between pressure drop and mass flow rate in a microchannel heat sink with rectangular channels. According to Stevens [7], this relation is given by equation (1), where $\dot{m}$ is the mass flow rate, μ the dynamic viscosity of the coolant, L the length of the channels, Po the Poiseuille number, ρ the mass density of the coolant, n the number of channels in the heat sink and D the hydraulic diameter of the channels:

$$\Delta p_f = \frac{\mu L \mathrm{Po}}{2\rho n D^4} \cdot \dot{m}. \tag{1}$$

The total thermal resistance R_{tot} is the sum of the caloric R_{cal} and the convective resistance R_{conv}. It is defined as the ratio of the maximal temperature difference to the total heat dissipation:

$$R_{\mathrm{tot}} = R_{\mathrm{cal}} + R_{\mathrm{conv}} = \frac{T_{w,\max} - T_{f,\mathrm{in}}}{Q}, \tag{2}$$

where $T_{w,\max}$ is the maximum temperature on the heat sink walls, $T_{f,\mathrm{in}}$ is the coolant temperature at the inlet and Q is the total heat load taken by the heat sink.

Figure 7 shows the analytical result for the thermal resistance of the heat sink as a function of varying channel aspect ratio. These calculations are performed for 450 μm deep channels which spread over a width of 12 mm and have a length of 12 mm, and using water as cooling fluid. The optimal thermal resistance is achieved at a channel aspect ratio of 5.6. Because of limitations in tool length versus tool diameter for small tools, the aspect ratio of the heat sink channels is limited to a factor 3. This leads to a decrease of performance from an optimal thermal resistance of 0.068 m^2 K W^{-1} to a thermal resistance of 0.103 m^2 K W^{-1}, and a pressure drop along the heat sink of 0.6 bar.

2.6. Heat sink wall thickness optimization

Optimization is also required for the channel wall thickness. If the fin width is too large, the heat transfer is decreased by the reduced area in contact with the cooling fluid. If the fin is too thin, the heat cannot pass through it and the coolant cannot extract the heat.

The wall thickness optimization for the cooling channels is based on the following considerations: the heat removed

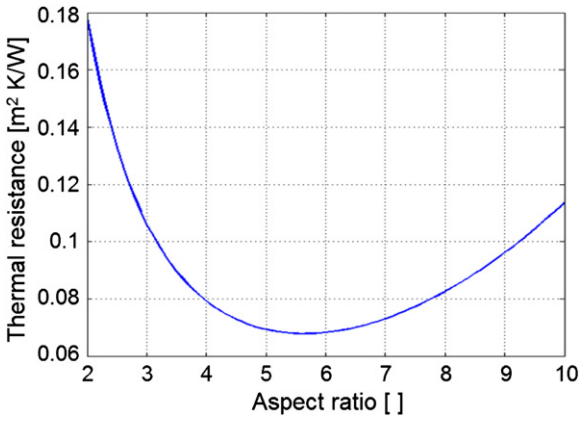

Figure 7. Thermal resistance of the heat sink in function of the channel aspect ratio.

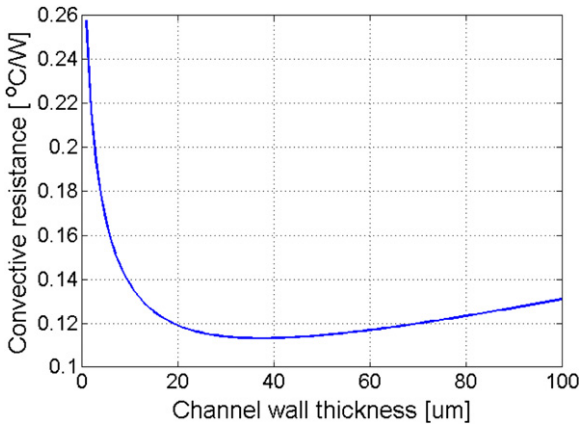

Figure 8. Convective resistance of the heat sink in function of the channel wall thickness.

by the heat sink Q is described by formula (3) as a product between heat sink efficiency η, the heat sink heat transfer coefficient k, the heat sink area in contact with the cooling fluid A and the cooling fluid temperature difference between the inlet and outlet ΔT:

$$Q = \eta \cdot h \cdot A \cdot \Delta T. \tag{3}$$

To increase the amount of heat removed by the heat sink we need to increase the area by adding more channels, and for that purpose the channel wall thickness has to be decreased in order to fit more channels on the heat sink.

The heat sink efficiency η is calculated with formula (4) where A_f is the area of the heat sink fins and η_f is the fin efficiency:

$$\eta = 1 - \frac{A_f}{A}(1 - \eta_f). \tag{4}$$

The fin efficiency is calculated with formula (5) [24], and h_{ch} represents the height of the fins. Parameter m is calculated with formula (6) [24], where k_f represents the fin conductivity and h_f the fin heat transfer coefficient:

$$\eta_f = \frac{\tanh(m \cdot h_{\mathrm{ch}})}{m \cdot h_{\mathrm{ch}}} \tag{5}$$

$$m = \sqrt{\frac{h_f \cdot P_f}{k_f \cdot A_f}}. \tag{6}$$

To increase the fin efficiency, m has to be minimized. Hence, the ratio between the perimeter P_f and the area A_f of the fin's cross-section has to be as small as possible. That means the heat sink wall thickness needs to be as large as possible. Thus, there is a trade-off for fin thickness, with thinner fins increasing heat transfer area and thicker fins improving heat sink efficiency. This results in an optimum fin width, as illustrated in figure 8, which plots the heat sink's convective resistance as a function of channel wall thickness, based on the above formulae.

As described in formula (3), the heat removal is increasing when the heat sink efficiency is increasing as well. Formula (7) indicates that for a smaller convective resistance R_{conv}, the heat sink efficiency has to also be higher:

$$R_{\mathrm{conv}} = \frac{1}{\eta \cdot h \cdot A}. \tag{7}$$

The value of h_f (1.42 W m^{-2} K^{-1}) is calculated from the Nusselt number determined in [25] for channels with aspect ratio 3 as used in this heat sink. The fin conductivity k_f is the conductivity of the material used for the heat sink (aluminium 7075) which is 130 W m^{-1} K^{-1}. The aluminium used for the heat sink material and the machining process makes it possible to produce channel wall thicknesses of 40 μm, very close to the optimum illustrated by figure 8.

3. Fabrication technology

The entire assembly is fabricated using micro-milling and micro-EDM technology. The material chosen for the metallic components is aluminium 7075. Besides its excellent thermal conductivity, its superior hardness makes it one of the best machinable materials (by milling) on the market, and allows aspect ratios up to 15 for heat sink fins.

The material used for the tube is Silastic Rx 50 medical grade tubing with an internal diameter of 0.51 mm and an external diameter of 0.94 mm. It was chosen because of its excellent flexibility (815% strain at failure) and tear strength (46 kN m^{-1}—CTM 0159A corresponding to American Standard Test Methods). It is non-reactive, stable, and resistant to extreme environments and temperatures from −55 °C to +300 °C while still maintaining its useful properties.

Expansion of the silicone tube at sections that do not contribute to the beam's actuation represents a loss in actuator stroke and should be minimized. Therefore, beneath the beam, the tube is placed between two ribs with a height of 0.5 mm that not only ensure proper positioning but also prevent the tube from expanding in horizontal direction. Furthermore, the non-contributing segments of the tube situated at the edges of the beam are reduced to a length of just 1 mm. For the rest of its length the tube is completely encapsulated. The amount of fluid expansion lost in this way represents just 5.7% of the total volumetric expansion of the oil. At the end of the tube, an empty groove of 3.5 mm long allows the tube to expand longitudinally under the influence of temperature and pressure.

Perfect sealing between the beam and the heat sink would require an ideal contact between them. This is not desirable because they need to have some play to avoid

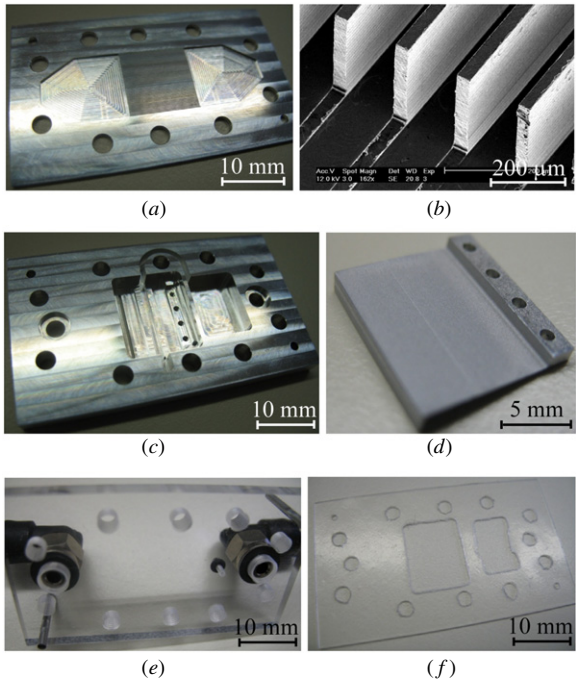

Figure 9. Thermopneumatic valve components: (*a*) heat sink, (*b*) cooling channels, (*c*) valve body with reservoir, (*d*) beam, (*e*) cover plate and (*f*) rubber gasket.

friction. Based on machining and aligning accuracy, this gap is 40 μm in our design. The material used for the beam is the same as for the heat sink, to avoid differential thermal expansion. The beam is fixed on the valve body with screws. The transversal alignment is done with the sides of the slot where the beam is attached. The temperature needed to open the valve is adjusted by heating up the reservoir to the required temperature with the filling orifice open so the excess of silicone oil can leave the reservoir. Before cooling down, the filling orifice is closed and sealed with a rubber o-ring around an M1 screw to avoid air entering the reservoir. The reasoning to choose a screw with such small dimensions is to avoid pressurizing the reservoir chamber and implicitly the tube while tightening the screw. The temperature operation range at which the valve is capable to operate is set by the melting and boiling points of the chosen silicone oil, which are respectively -26 °C and 101 °C. Figure 9 shows the main valve components.

The cover plate is chosen to be transparent to provide visual access to the inner working of the valve to monitor the beam deflection and to detect potential leakages. A material that provides transparency as well as machinability, mechanical strength and a melting point above the valve's maximum operating temperature is polycarbonate (PC). The heat sink and the valve body are screwed directly on the cover.

The tube is closed on one end with a silicone plug, while the other end is inserted in the reservoir via a circular groove. The circular groove is filled with a structural epoxy adhesive (3M DP110) to secure the tube and seal the groove.

A silicone rubber gasket, 0.5 mm in thickness is glued on the cover plate to avoid leakage between the reservoir and the valve chamber. Loctite 406 is used for gluing, in combination with a primer for surface activation (Loctite 770).

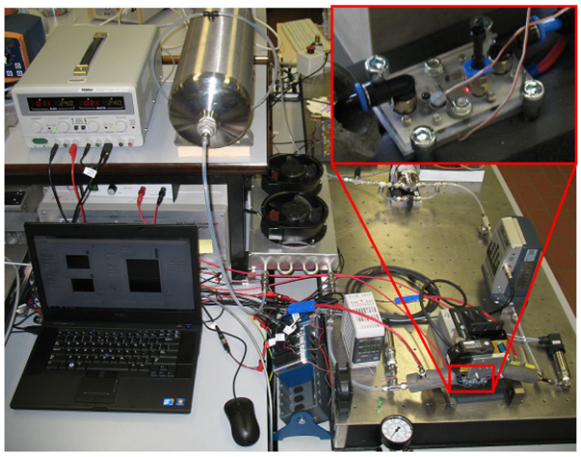

Figure 10. Test setup for valve characterization. The insert provides an enlarged view on the valve.

The PC cover plate also contains an orifice for inserting a thermocouple sensor into the reservoir. This thermocouple sensor is glued in a hole drilled axially through a plastic screw, and that screw is then mounted in the cover plate (see figure 3). Sealing is implemented by a rubber o-ring between the screw and the PC plate. That way, the temperature sensor can be interchanged with an external pressure supply, like compressed air, to determine the relationship between tube pressure and beam displacement, pressure drop and flow. The other orifice connectors for the inlet, outlet and the valve chamber are offering perfect sealing with the PC cover.

Figure 10 shows a picture with the complete measurement system where you can see the valve surrounded by the measurement instruments.

4. Measurement setup

Figure 11 gives a schematic representation of the measurement setup, also shown in figure 10. The cooling fluid is stored in a container (1). The opening and closing of the circuit is realized by valves (2) and (3) while the coolant flow is regulated by a gear pump (5) which is placed in parallel with a safety bypass controlled by a valve (4). The flow is measured with a flow meter (7), after passing through a 10 μm filter (6). The absolute pressure is measured with a pressure sensor (8) and the pressure drop across the valve and heat sink (9) with a differential pressure sensor (17). The valve inlet temperature is measured by a thermocouple (13) and the outlet with another thermocouple (16). A thermocouple (15) is inserted in the valve reservoir to read the temperature of the silicone oil. The valve deflection is determined with a laser displacement system (14) which uses the method of laser beam triangulation. The temperature of the heating resistor (10) is controlled by the power source (11) using feedback from a thermocouple (12) placed at the junction between the heat sink and the heater. The ambient temperature is maintained at 20.5 °C.

Table 3 illustrates the type, model, resolution and range of the measurement instruments. Data acquisition and control of

Table 3. Characteristics of the measurement instruments.

Type	Model	Measured variable	Resolution	Measurement range
Laser distance sensor	Keyence LK-G32	Beam deflection	0.1 μm	$\pm$5 mm
	Keyence LK-3001PV	Controller	0.01 μm	–
	Baumer S35 A	Beam deflection	4 μm	$\pm$1 mm
Absolute pressure sensor	Druck UNIK 5000	Inlet pressure	0.002 bar	$-$1–4 bar
Differential pressure sensor	Druck UNIK 5000	Inlet to outlet pressure difference	0.001 bar	0–3 bar
Flow meter	Cori-flow	Coolant flow rate	0.02 Kg h^{-1}	0–50 Kg h^{-1}
Temperature sensor	Omega PFA T-type	Coolant temperature at inlet and outlet	0.2 °C	0–205 °C
Temperature sensor	Thermocouple J-type	Heater, silicone oil temperature	0.1 °C	0–100 °C

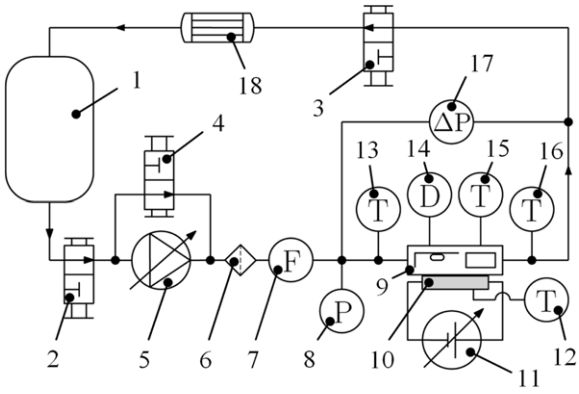

Figure 11. Schematic representation of the measurement setup.

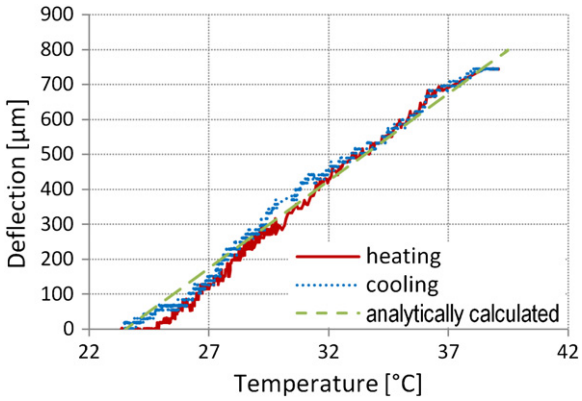

Figure 12. Beam deflection versus temperature at atmospheric pressure.

the measurement setup was performed by a real-time controller from National Instruments, NI cRIO-9074. The measurement instrument's resolution displayed in table 3 is the resolution obtained after conversion from analogue to digital signal.

5. Measurements

5.1. Beam characterization

5.1.1. Actuation capability

Experiment description. As the actuation of the beam is central to the operation of the valve, beam deflection was measured as a function of temperature (figure 12). The measurements were taken at an ambient temperature of 23 °C and zero flow rate (dry measurement). The plotted temperature is the average between the temperature measured in the silicone oil reservoir and the temperature measured at the junction between the heat sink and heater. The heater is a heating resistor, used to simulate the heat generated by the IC. The reservoir volume was 350 mm^3; thus, the valve beam that regulates the flow should achieve a stroke of 500 μm over a temperature range of 10 °C (see table 1). This stroke should be sufficient to completely expose the channels which are 450 μm high. The beam deflection was measured with a Baumer S35A laser triangulation sensor, having a resolution of 4 μm.

Experimental result. As can be seen in figure 12, a stroke of 500 μm is observed for a temperature difference of 10 °C, ensuring the valve is completely open. As the temperature increases further, the measurement shows that the beam is capable of reaching even higher deflections of up to 745 μm at a 15 °C temperature difference. When temperature decreases, the hysteresis shown is insignificant. At the end of the measurement, the beam position reached the same height as at the beginning, showing that the beam has not been plastically deformed. It can be observed that the beam deflection is linear with the temperature over the entire stroke. This feature allows the valve to regulate the flow linearly with the temperature, offering an important advantage in cooling rate stability.

The conclusion of this measurement is that the measured stroke is more than sufficient compared to the 450 μm channel height, ensuring a zero increase in pressure drop at complete opening.

5.1.2. Pressure drop sensitivity. When placed in a flow loop, the flow pressure has an influence on the beam position. As was described in the design and operating principle section, the force associated with the pressure drop across the gate is causing a downwards bending moment on this gate towards the closing position.

Experiment description. In these measurements and all the measurements that follow, the valve is placed in the cooling circuit using distilled water as coolant.

The pressure drop across the beam was determined from the difference between the measured pressure drop across the valve and heat sink when the valve action was used, and the measured pressure drop across valve and heat sink when the beam was removed. A constant external pressure of 1.5 bar was applied in the tube, pushing up the beam 230 μm from the channel base. The flow rate was increased until the pressure

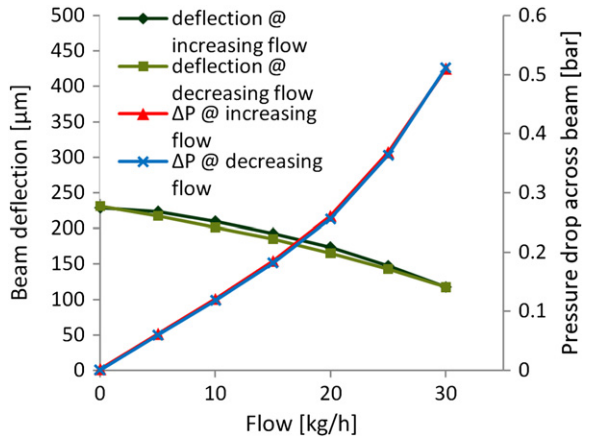

Figure 13. Beam deflection and pressure drop versus flow rate at reservoir pressure of 1.5 bar.

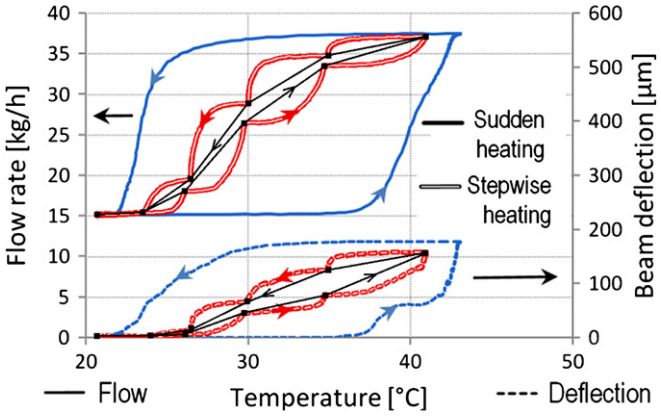

Figure 14. Flow rate and beam deflection versus heater temperature at a ΔP of 0.5 bar.

drop across the valve reached 0.5 bar. For this measurement and for all the measurements that follow, beam deflection was measured with the laser distance sensor 'Keyence LK-G32' with accompanying controller 'Keyence LK-3001PV'. The reason for this is that these experiments are performed on the valve surrounded by the cooling fluid and that this sensor is capable to measure the beam deflection without being influenced by the polycarbonate cover plate and the layer of water in between.

Experimental result. The effect of the flow rate on the pressure drop across the gate and the resulting beam deflection were measured and plotted in figure 13.

As expected, the beam moved downwards linearly with the pressure drop across it. From this measurement it can be concluded that the flow rate causes a deflection of 112 μm at maximum pressure drop, or 22.3% of the 500 μm stroke. It is very close to the prediction of 17.4% made by numerical simulations for the same pressure drop across the beam (0.5 bar) and the same starting beam deflection (230 μm).

5.2. Valve characterization

5.2.1. Valve flow rate regulation as function of temperature

Experiment description. In these measurements, the thermal properties of the valve were investigated. For this purpose, the pump regulates the flow in function of the valve behaviour in such way that the pressure difference between inlet and outlet is kept constant.

In a first experiment, a sudden power input of 490 W is applied to the heater for 6 min, followed by another 6 min of cooling at zero power input. In a second experiment, the heat is applied stepwise: 0, 13, 50, 113, 202, 315 and 450 W with time intervals of 2 min. The same procedure is used during cooling. A pressure drop of 0.5 bar is maintained across the valve and heat sink.

Experimental result. Figure 14 shows the resulting flow rate and beam deflection as a function of heater temperature. The displayed temperature is the temperature measured on the heater (IC).

For sudden heating, large hysteresis can be observed on the beam deflection and the flow rate. This can be explained by the large thermal mass of the heat sink. For stepwise heating the system reached a state closer to equilibrium at intermediate steps, thus, much lower hysterisis. The beam did not reach the maximum deflection of 500 μm because the temperature of the actuation fluid (silicone oil) had increased by only 4 °C due to the strong cooling. It can be observed that the valve did not fully block the flow in the closed position because of the 40 μm gap between the beam and the heat sink which is used to prevent friction. The steady-state response of the valve to a certain heat load is approximated by the lines with square markers. The markers represent the values at the end of each step, when the system has found a new equilibrium. The remaining hysteresis is caused by the limited waiting time between heat input changes (2 min). The heater reaches a 9% higher temperature difference between the start and the end of the measurement for sudden heating because the power input is 9% higher than for gradual heating (limits set by the power amplifier).

5.2.2. Dynamic response

Experiment description. The experimental conditions are the same as for the previous experiment in section 5.2.1: heat is applied stepwise from 0 to 450 W and back with 2 min waiting time for each step. Also the power levels are the same as in the previous experiment. During the measurements, the pressure drops were maintained constant such that the flow rate was increasing as the valve was opening.

For comparison, the same measurement was performed on the valve in the closed state and in the fully opened state. The valve was maintained in the closed state by keeping the reservoir filling orifice open such that the actuation fluid remained at ambient pressure and was not able to lift the beam. The constantly open state was realized by externally applying a constant and sufficiently high pressure (3 bar) on the reservoir.

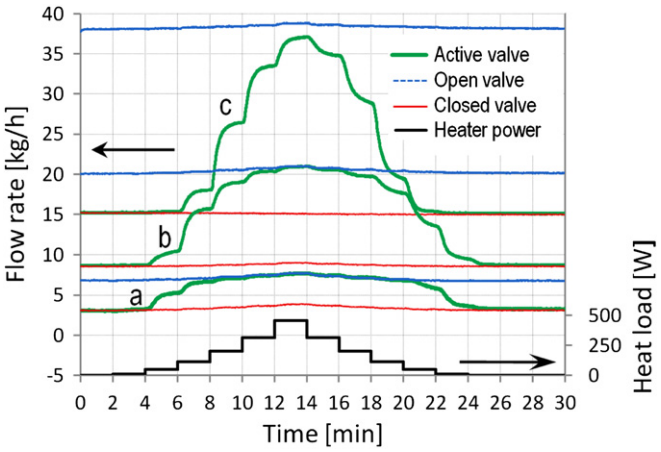

Figure 15. Flow rate in function of time for a stepped heat input at ΔP 0.05 (*a*), 0.2 (*b*) and 0.5 bar (*c*).

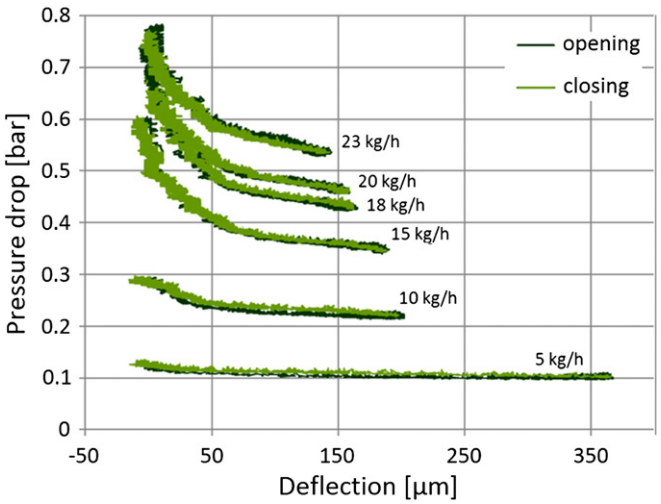

Figure 16. Pressure drop versus deflection.

Experimental result. Figure 15 displays the flow rate as a function of time as the heat load changes stepwise, and this for pressure drops of 0.05, 0.2 and 0.5 bar.

The experiments with sudden heating indicate a reaction time of 10 s, due to the time required to heat the oil in the reservoir. A similar response is observed for the stepwise heating, but with smaller hysteresis, as the system gets time to adapt to the new temperature at each step.

It can be observed that the valve was able to regulate the flow over the full range and to completely close every time. At the highest flow rate however, when ΔP equals 0.5 bar, the maximum flow rate could not be achieved by a small margin due to the too strong cooling that prevented the silicone oil to heat up enough. It has been observed that the heat sink flow resistance increases with the flow such that, above a certain flow rate, the pressure drop caused by the beam is negligible in comparison to the total pressure drop. For a flow rate of 38 kg h^{-1}, it occurs at a pressure drop of 0.5 bar when the beam is in open position, the stroke required is just 170 μm, compared to the 450 μm of the channel height.

The thermal and mechanical deformation of the tube are insignificant factors for the reaction time of the valve, because

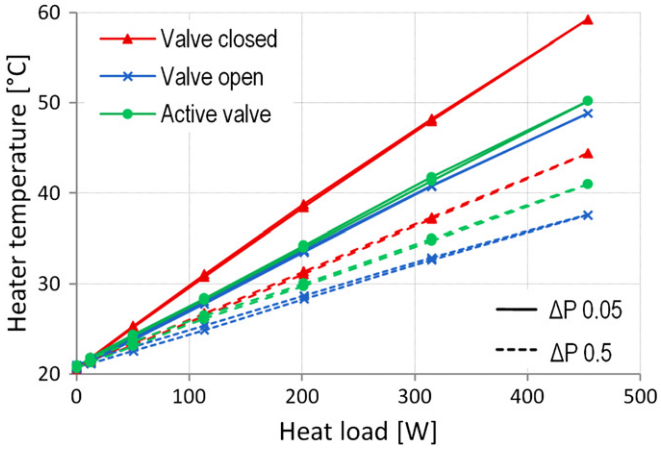

Figure 17. Heater temperature versus heat load.

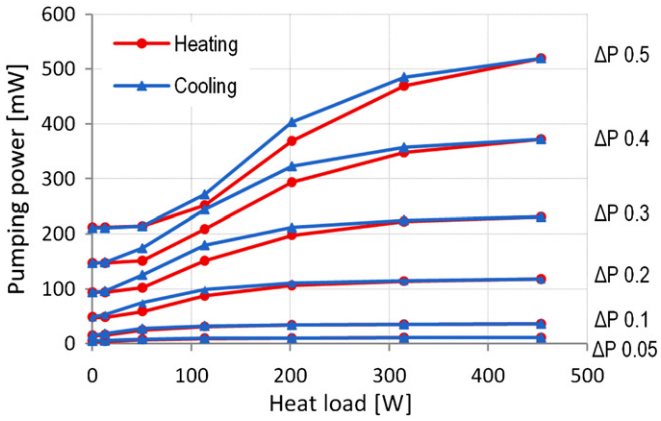

Figure 18. Pumping power versus heat load.

the oil volume in the silicone tube remains below 1.3% of the total oil volume under all conditions of pressure and temperature. Thus, the dominant time delay originates from the thermal inertia of the oil in the reservoir, and the thermal resistance of the path from the heater (IC) to this oil.

5.2.3. Pressure drop

Experiment description. In this test, the flow rate was maintained constant while the pressure drop varied in function of the valve opening. A sudden power input was applied to the heater to open the valve, followed by a cooling period after the power input was stopped to close the valve.

Experimental result. Figure 16 presents the pressure drop across the valve as a function of deflection for different flow rates.

For high flow rates, the beam deflection is limited because the cooling becomes too strong for the current heater. For low flow rates, beam deflection seems to have an almost negligible effect on the pressure drop, while for high flow rates more variation in pressure drop is observed. The absence of hysteresis in this measurement suggests that the hysteresis shown in the previous measurements in not caused by the flow characteristics of the valve.

5.2.4. Cooling performance

Experiment description. In these experiments, the measurements were performed under the same conditions as for the ones in section 5.2.2. The heater temperature is measured at the junction with the heat sink. The heat load is applied stepwise as described in the previous experiments. Pressure drop is kept constant at 0.05 or 0.5 bar. Measurements on closed and open valves are added for comparison.

Experimental result. In figure 17, the heater temperature is plotted in function of the heat load applied to it. The measurement points displayed on the graph are the equilibrium values reached after a period of 2 min.

At smaller flow rates, the heat removal is lower and thus the heater temperature is higher. For the low-pressure drop of 0.05 bar (corresponding to low flow rates), the temperature of the active valve follows very closely the characteristic of the constantly open valve for almost the entire range. This is very logical since the overheated valve is craving for cooling fluid and will open completely. For high flow rates ($\Delta P = 0.5$ bar), the active valve follows the trend of the closed valve at heat inputs up to 100 W, and then acts halfway between the open and closed characteristics.

The developed cooling system achieved a better cooling performance than set forth in the specifications (500 W cm^{-2} for a ΔT of 35–40 °C), managing to absorb a heat flux of 450 W cm^{-2} for gradual power input at a temperature difference of 21 °C and 490 W cm^{-2} for sudden power input at a temperature difference of 23 °C.

5.2.5. Power saving performance

Experiment description. An interesting characteristic and decisive factor for using valves in single-phase cooling is the pumping power saving performance. As for the experiments described in sections 5.2.1, 5.2.2 and 5.2.4, a stepwise heat load was applied on the valve with the same waiting time of 2 min between the measurements. While a constant pressure drop between 0.05 and 0.5 bar was maintained across the valve, flow rate and pumping power varied as the valve opened and closed in response to the varying heat input.

Experimental result. If there was no valve to control the flow, the pumping power would be the same for each heat load. Using a valve, at low heat loads, the flow can now be reduced contributing to the saving of pumping power. Depending on the pressure drop set across the valve, the saved pumping power amounts to up to 320 mW, corresponding to 60% power savings as shown in figure 18. The hysteresis is a measurement artefact caused by insufficient settling time (2 min) preceding the individual measurements.

6. Conclusion

Thermal cycling is one of the main factors influencing the lifetime and computational power of electronic devices. The thermopneumatic valve shows a novel actuation principle that combines the advantages of zero power consumption, small size versus high flow rate and low manufacturing costs. Its independence from external energy makes it suited for portable devices. Its passive operation increases the simplicity and reliability. It uses an inherent feedback mechanism that allows proportional flow control in function of the power dissipated by the IC. Measurements confirmed the beam actuation capabilities and demonstrated that the flow can be effectively controlled. After actuation, the beam returns to the start position after each cycle. However, due to the long thermal path and the large thermal inertia of the oil reservoir, the valve response time is greatly increased. An actuation fluid capable of changing its phase from liquid to gas would significantly increase the actuation speed because the volumetric expansion would be highly amplified and thus a much smaller amount of actuation fluid would be required. A smaller volume leads to a smaller heat capacity and thus higher speeds. Although phase transformation requires a high amount of energy, the greatly reduced mass of actuation fluid in combination with a much higher relative contact surface would substantially improve the valve reaction times. The cooling capabilities have been demonstrated by achieving a heat load removal of 490 W at a temperature difference of only 23 °C. This valve can be used together with any heat sink used for microelectronics cooling. It has the capability of maintaining a more uniform IC temperature which increases the IC lifetime, and at the same time, it saves up to 60% pumping power.

Acknowledgments

This research is sponsored by IWT, the Institute for the Promotion of Innovation by Science and Technology—Flanders, Belgium; project SBO ‘HyperCool-IT’.

References

[1] Kraus A D and Bar-Cohen A 1983 *Thermal Analysis and Control of Electronic Equipment* (New York: Hemisphere) pp 620
[2] Bar-Cohen A and Kraus A D 1988 *Advances in Thermal Modelling of Electronic Components and Systems* (New York: Hemisphere) pp 450
[3] Yeh L Y and Chu R C 2002 *Thermal Management of Microelectronic Equipment* (New York: ASME Press) pp 440
[4] Garimella S V 2006 Advances in mesoscale thermal management technologies for microelectronics *Microelectron. J.* **37** 1165–85
[5] Patterson M K and Fenwick D 2008 A review of current air and liquid cooling solutions White Paper—The State of Data Center Cooling Intel Corporation pp 12
[6] Singhal V, Garimella S V and Raman A 2004 Microscale pumping technologies for microchannel cooling systems *Appl. Mech. Rev.* **57** 191–221
[7] Stevens T 2008 Design methodologies for efficient heat transfer in micro systems *PhD Thesis* Katholieke Universiteit Leuven
[8] Oh Kwang W and Ahn Chong H 2006 A review of microvalves *J. Micromech. Microeng.* **16** R13–39
[9] Moers T 2010 Development of a surgical manipulator with integrated microhydraulic actuation and control *PhD Thesis* Katholieke Universiteit Leuven

[10] Dong S, Du X, Bouchilloux P and Uchino K 2002 Piezoelectric ring-morph actuator for valve application *J. Electroceram.* **8** 155–61
[11] Clausi D, Gradin H, Braun S, Peirs J, Stemme G, Reynaerts D and van der Wijngaart W 2010 Design and wafer-level fabrication of SMA wire microactuators on silicon *J. Microelectromech. Syst.* **19** 982–91
[12] Clausi D, Gradin H, Braun S, Peirs J, Reynaerts D, Stemme G and van der Wijngaart W 2011 Wafer-level mechanical and electrical integration of SMA wires to silicon MEMS using electroplating *Proc. IEEE MEMS 2011* pp 1281–4
[13] Peirs J, Reynaerts D and Van Brussel H 2002 A retrospective evaluation of SMA micro-actuation *Proc. 8th Int. Conf. on New Actuators* pp 77–80
[14] Peirs J, Reynaerts D and Van Brussel H 2001 The 'true' power of SMA micro-actuation *Proc. 12th Micromechanics Europe Workshop MME 2001* pp 217–20
[15] Reynaerts D, Peirs J and Van Brussel H 1995 Production of shape memory alloys for microactuation *J. Micromech. Microeng.* **5** 150–2
[16] DeVolder M *et al* 2006 The use of liquid crystals as electrorheological fluids in microsystems: model and measurements *J. Micromech. Microeng.* **16** 612–9
[17] Charles S W 2002 *Ferrofluids: Magnetically Controllable Fluids and Their Applications* (Lecture Notes in Physics) (New York: Springer) pp 3–18
[18] Charles S W 1995 Preparation and magnetic properties of magnetic fluids *Rom. Rep. Phys.* **47** 249–64
[19] Richter A, Kuckling D, Howitz S, Gehring T and Arndt K F 2003 Electronically controllable microvalves based on smart hydrogels: magnitudes and potential applications *J. Microelectromech. Syst.* **12** 748–53
[20] http://www.gesim.de/upload/PDFs/Hydrogel_Valve.pdf Hydrogel Valves—Dead-Volume-Free Microfluidic Switches. Data sheet 2007: downloaded at 25/02/2011
[21] De Volder M and Reynaerts D 2010 Pneumatic and hydraulic microactuators: a review *J. Micromech. Microeng.* **20** 043001
[22] Smal O, Dehez B, Raucent B, De Volder M, Peirs J, Reynaerts D, Ceyssens F, Coosemans J and Puers R 2008 Modeling, characterization and testing of an ortho-planar micro-valve *J. Micro-Nano Mech.* **4** 131–43
[23] Mayhew Jr and John D 1983 Knife gate valve *US Patent* US4377274
[24] Incropera F and De Witt D 1990 *Fundamentals of Heat and Mass Transfer* 3rd edn (New York: Wiley) pp 919
[25] Shah R K and London A L 1978 *Laminar Flow Forced Convection in Ducts* (New York: Academic) pp 477